

STAT

31 August 1964
RK:bb:406
(997-112)

MEMORANDUM FOR THE RECORD

STAT

By:
Subject: Influence of Coherence Upon Images in the Microdensitometer
CC:

STAT

INTRODUCTION

This memo reports the results from several investigations which have been undertaken on Project Microcap¹ since a previous memo.² The areas investigated include: 1) edge objects possessing finite resolution, in particular trapezoidal objects, 2) theoretical evaluation of the modulation transfer functions determined from sine-wave test charts and edge traces, and 3) the use of a coherent light source (laser) in the microdensitometer including the influence of the width of the illuminating slit.

The reason for investigating trapezoidal objects is simply that sharp edges do not occur in real test objects used in the microdensitometer and, consequently, it is desirable to confirm the conclusions stated in the previous memo for edge objects having a finite resolution.

In current usages a microdensitometer usually employs partially coherent illumination of the test object. Consequently, the usual methods of forming the MTF (modulation transfer function), i. e., from edge traces or sine-wave test charts, are not valid and at best can be considered a useful approximation. The

¹ Unless it is indicated otherwise.

STAT

² Results of Theoretical Studies of the Influence of the Degree of Coherence Upon Images of Edges, RK:bb:283, 22 June 1964, Revised-9 July 1964.

purpose of the investigation in this area was to determine what theoretical results can be expected from both methods and to determine if both methods yield similar results.

The final area of investigation reported in this memo was performed with the intent of gaining information about two problems simultaneously. These problems concern the consequences upon edge traces of employing a laser source (coherent source) and the influence of width of the illuminating slit upon the microdensitometer output. When the illuminating slit becomes small (i. e., comparable to the diffraction limit of the microscope), the microdensitometer is no longer an imaging system so that changes in its output are possible.

Each of these investigations will be discussed in more detail in the following sections.

TRAPEZOIDAL OBJECTS

The amplitude transmittance of this object is assumed to be:

$$T(u) = \begin{cases} 0 & u \leq 0 \\ \frac{Au}{S} & 0 \leq u \leq S \\ A & S \leq u \leq w+S \\ \frac{A}{S}(w+2S-u) & w+S \leq u \leq w+2S \\ 0 & w+2S \leq u \end{cases} \quad (1)$$

Figure 1 is a graph of the intensity transmittance of this object. The corresponding object amplitude spectrum is

$$O(m,n) = \frac{2A}{S} \delta(n) \left\{ \frac{\cos\left[\left(\frac{w}{2}\right)m\right] - \cos\left[\left(\frac{w}{2}+S\right)m\right]}{m^2} \right\} e^{i\left(\frac{w}{2}+S\right)m} \quad (2)$$

Following the procedure outlined in the previous memo,² the intensity in the image may be found by performing two integrations. As in all the previous cases, the final integration involves sine and cosine integral functions and must be done numerically. In this case³, this integral has the form:

$$I'(u') = K \int_{-\epsilon}^{\epsilon} \left\{ \left[\text{Re}(\phi) \right]^2 + \left[\text{Im}(\phi) \right]^2 \right\} d\gamma \quad (3)$$

³ For convenience the system is assumed to possess square apertures and square effective sources, i. e., $f(x,y) = 1$ for $|x| \leq 1, |y| \leq 1$ and $A(x,y) = \frac{1}{2\pi}$ for $|x| \leq \epsilon, |y| \leq \epsilon$

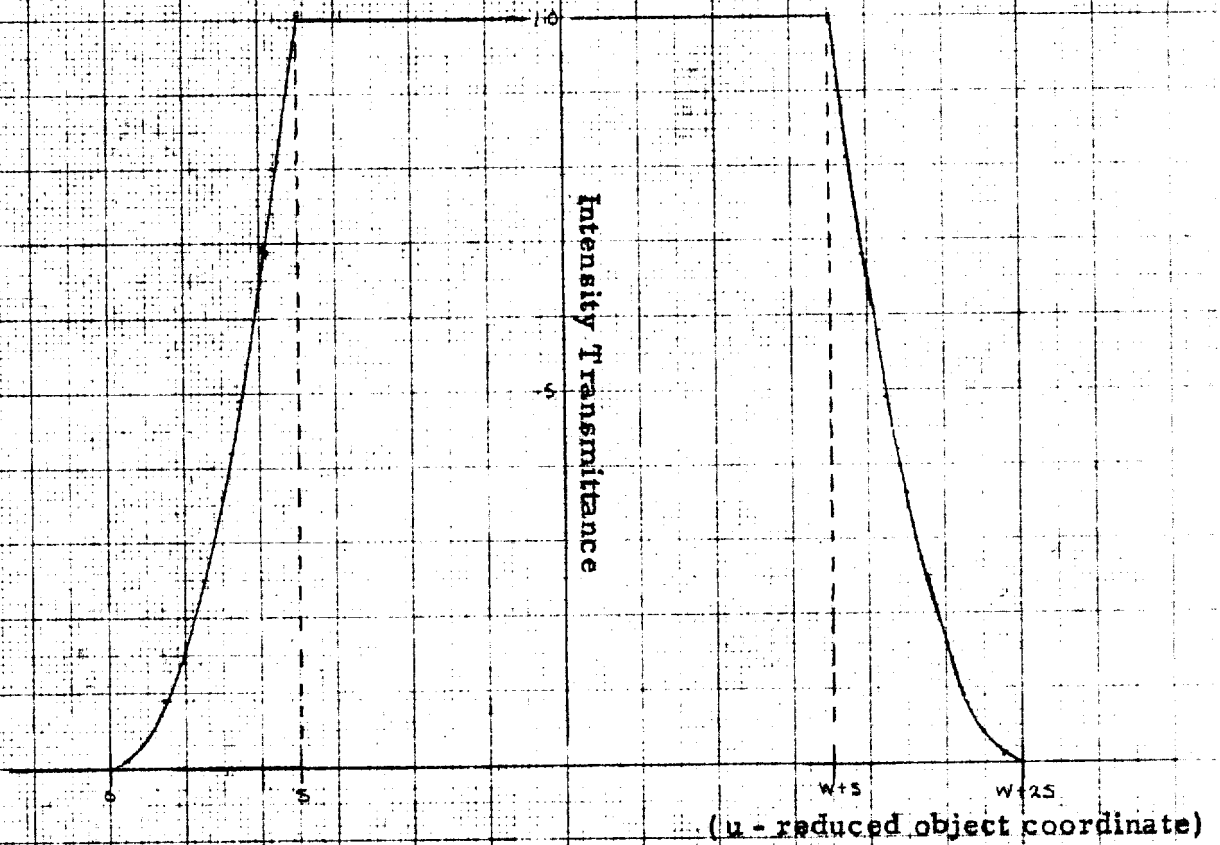


FIGURE 1

Intensity Transmittance for a Trapezoidal Object

where

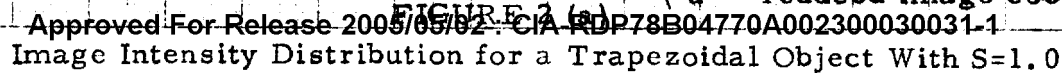
$$\begin{aligned}
 \text{Re}(\phi) = & \frac{2 \cos \left[\frac{W+2S}{2} - u' \right] [1-x] \sin \left[\frac{W+S}{2} \right] [1-x] \sin \frac{S}{2} [1-x]}{1-x} \\
 & + \frac{2 \cos \left[\frac{W+2S}{2} - u' \right] [1+x] \sin \left[\frac{W+S}{2} \right] [1+x] \sin \frac{S}{2} [1+x]}{1+x} \\
 & + \frac{1}{2} \left\{ [W+2S-u'] \text{Si} [W+2S-u'] [1-x] + u' \text{Si} u' [1-x] - [W+S-u'] \text{Si} [W+S-u'] [1-x] \right. \\
 & - [u'-S] \text{Si} [u'-S] [1-x] + [W+2S-u'] \text{Si} [W+2S-u'] [1+x] + u' \text{Si} u' [1+x] \\
 & \left. - [W+S-u'] \text{Si} [W+S-u'] [1+x] - [u'-S] \text{Si} [u'-S] [1+x] \right\}
 \end{aligned}$$

and

$$\begin{aligned}
 \text{Im}(\phi) = & \frac{2 \sin \left[\frac{W+2S}{2} - u' \right] [1-x] \sin \left[\frac{W+S}{2} \right] [1-x] \sin \frac{S}{2} [1-x]}{1-x} \\
 & - \frac{2 \sin \left[\frac{W+2S}{2} - u' \right] [1+x] \sin \left[\frac{W+S}{2} \right] [1+x] \sin \frac{S}{2} [1+x]}{1+x} \\
 & + \frac{1}{2} \left\{ [u'-(W+S)] \text{Ci} [u'-(W+S)] [1-x] + [u'-S] \text{Ci} [u'-S] [1-x] - [u'-(W+2S)] \text{Ci} [u'-(W+2S)] [1-x] \right. \\
 & - u' \text{Ci} u' [1-x] - [u'-(W+S)] \text{Ci} [u'-(W+S)] [1+x] - [u'-S] \text{Ci} [u'-S] [1+x] \\
 & \left. + [u'-(W+2S)] \text{Ci} [u'-(W+2S)] [1+x] + u' \text{Ci} u' [1+x] \right\}
 \end{aligned}$$

The intensity distributions were computed⁴ for values of S=1.0, 4.25 and 10.0. These results for varying degrees of coherence (i.e., ratio of numerical apertures of the condenser to the analytical objective) are shown in Figure 2 (a), (b), and (c) respectively. As before, the expanded scale is also shown to indicate the changes which occur in the edgegradients (Figure 3 (a), (b), and (c)). The results support identical conclusions for finite resolution edge that were previously reported for sharp edged objects. In addition, it is noticed that amplitude of the ringing decreases as the object becomes less sharp (i.e., larger S value) which is to be expected.

⁴ Several of these cases were computed under
Internal Research Report No. 86-139.



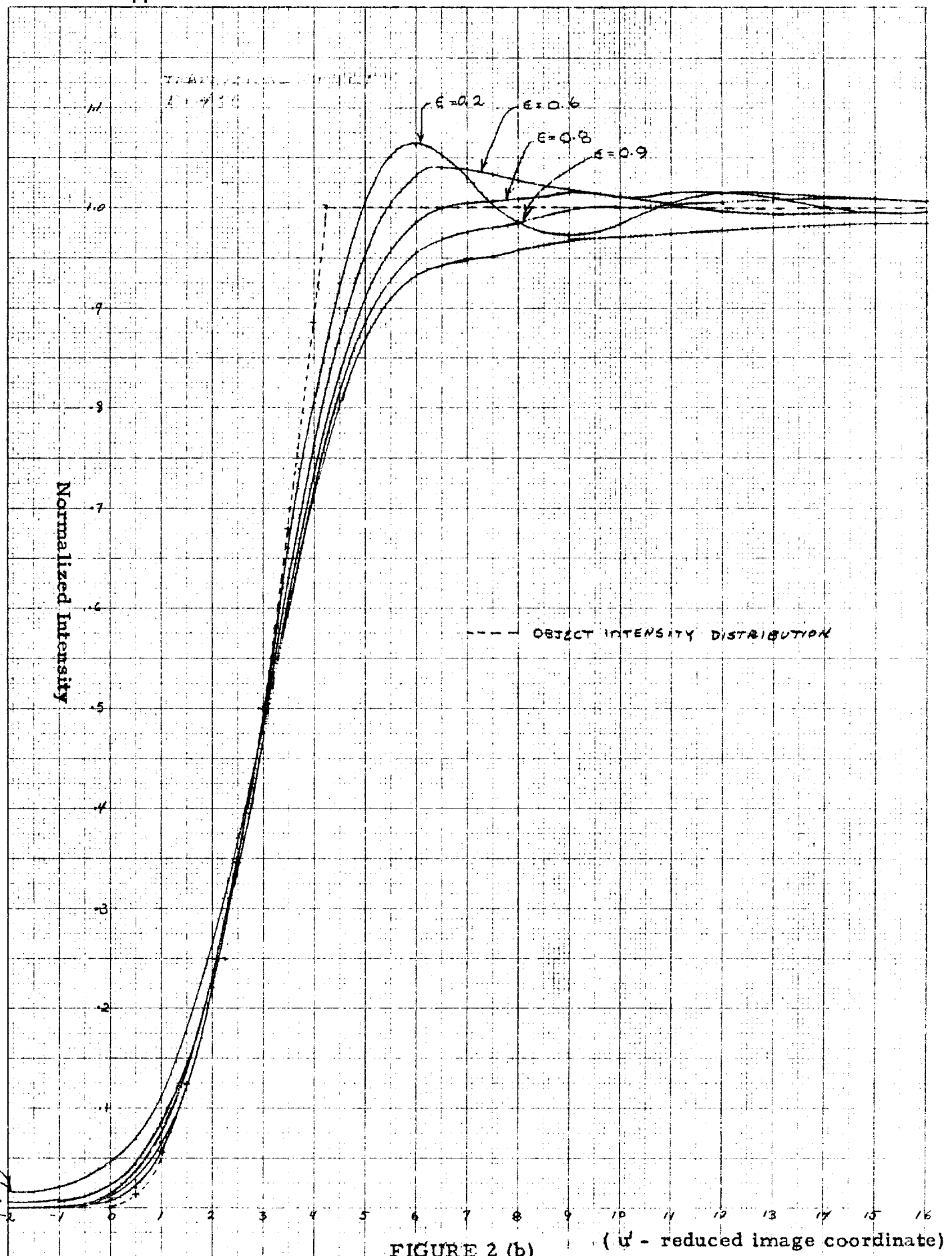


FIGURE 2 (b)

(u' - reduced image coordinate)

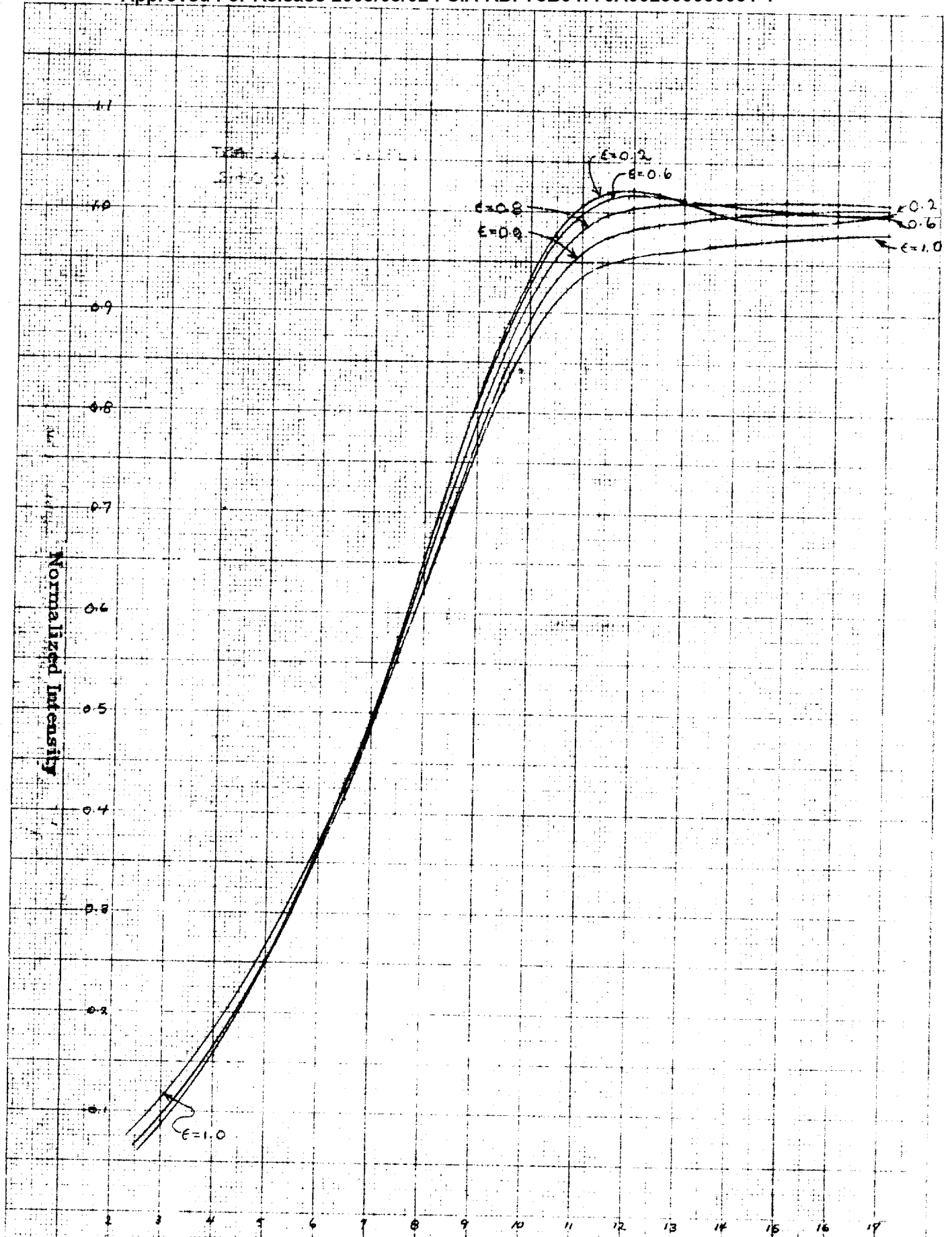
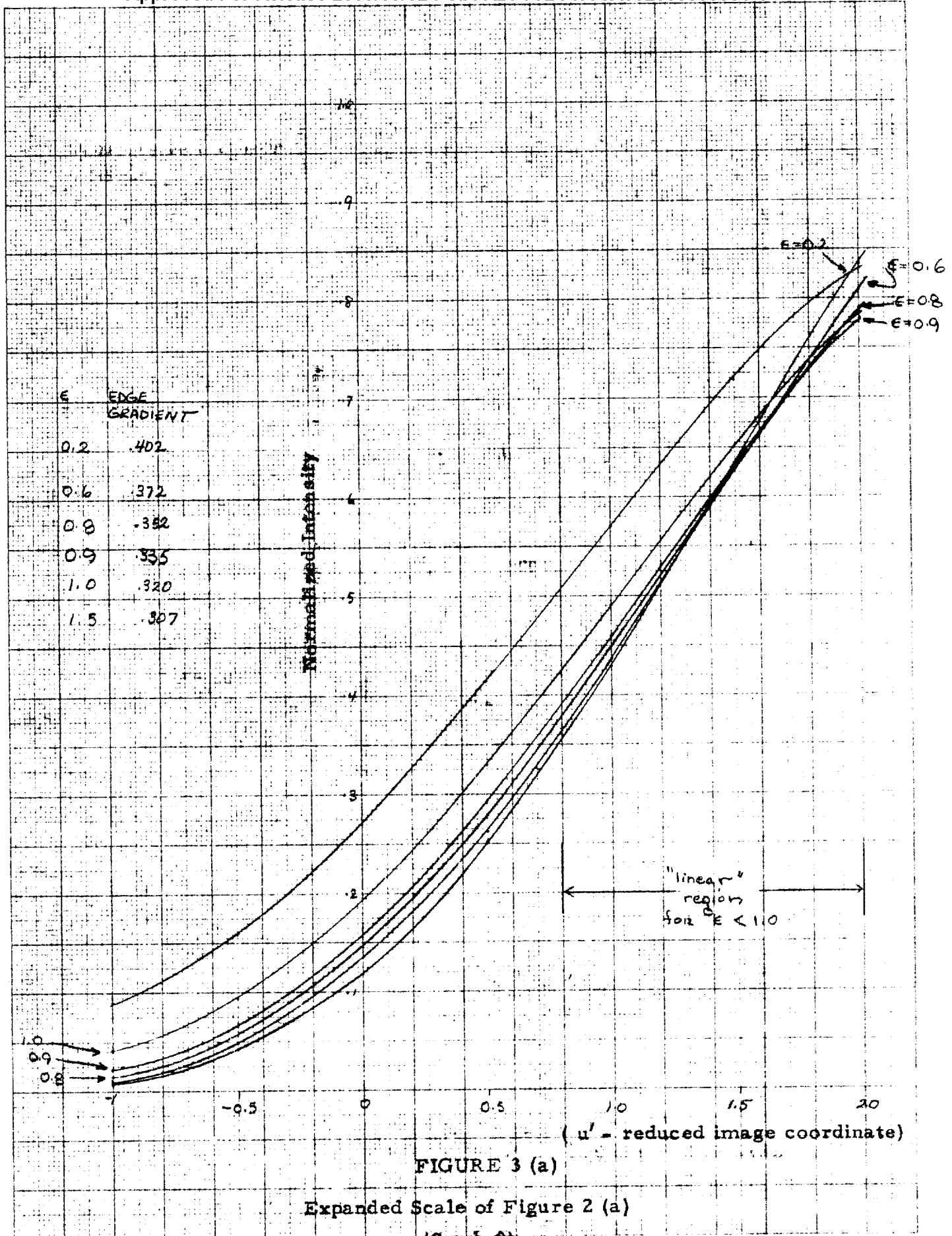
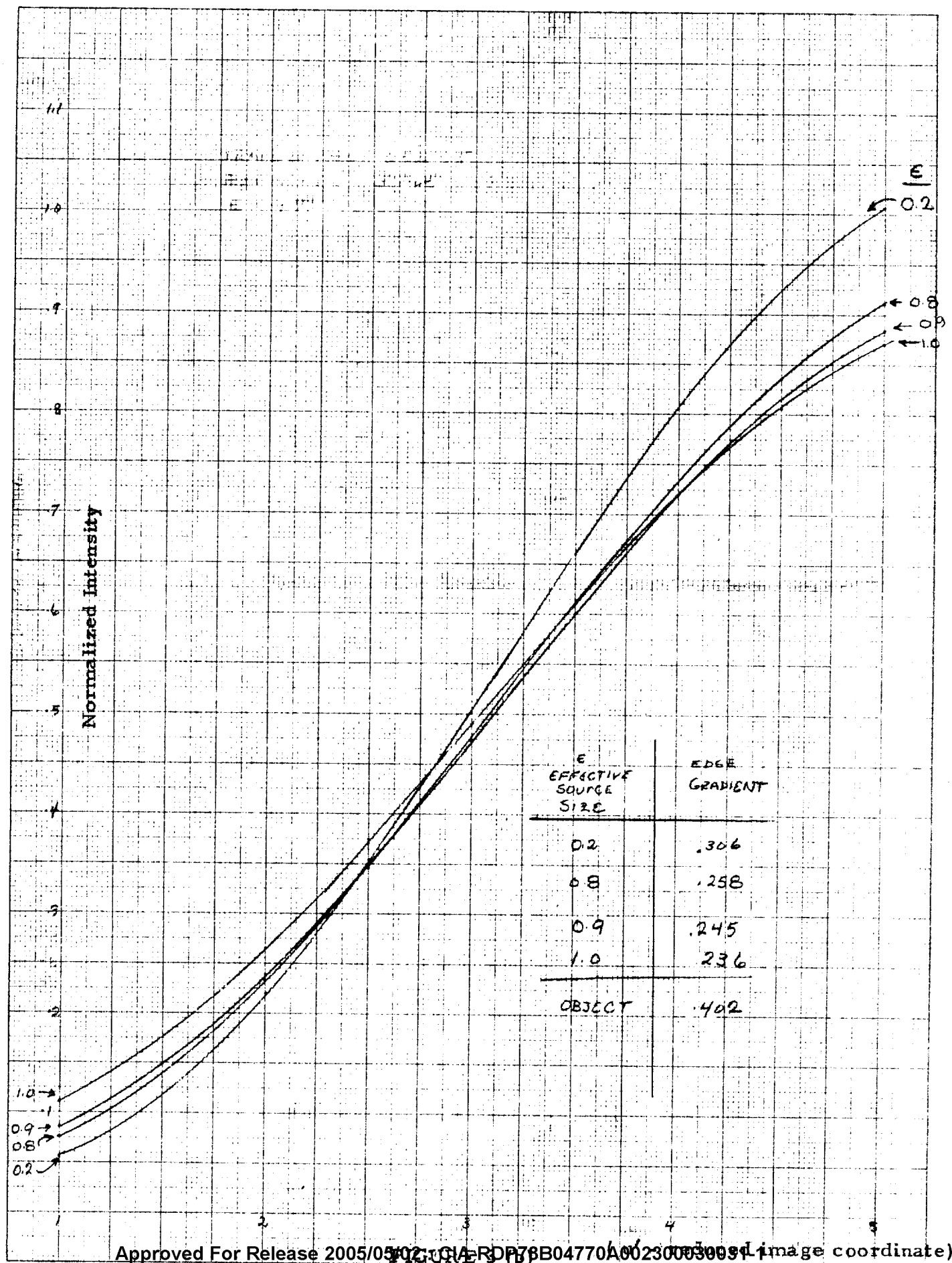


FIGURE 2(c) (u' - reduced image coordinate)

NO INSTR. MP. GRAPH. PAPER
MILLIMETER

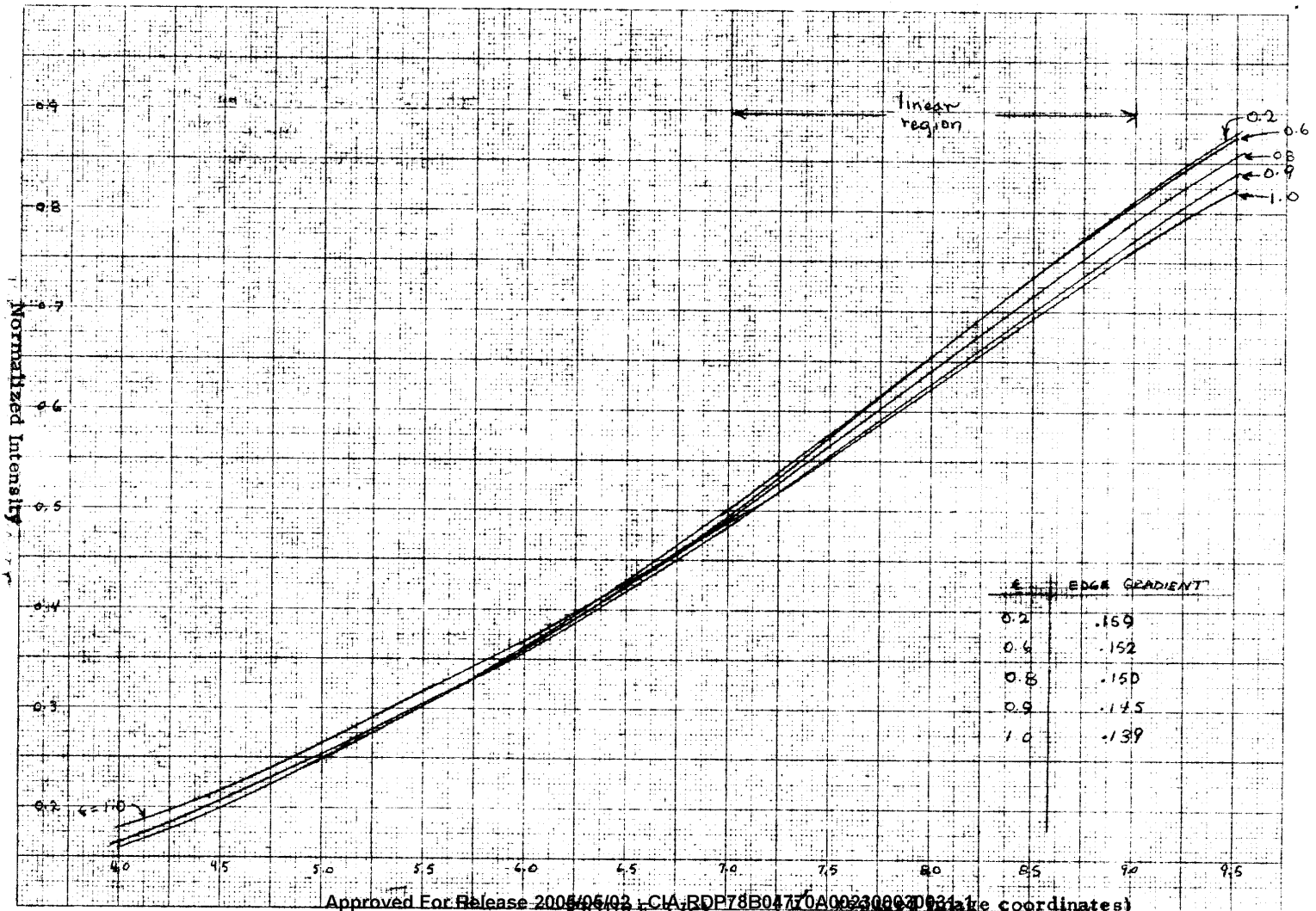




NO 15TR MP GRAPH PAPER
MILLIMETER

VISIGRAPH
MADE IN U.S.A.

Approved For Release 2005/05/02 : CIA-RDP78B04770A002300030031-1



Approved For Release 2005/05/02 : CIA-RDP78B04770A002300030031-1

Expanded Scale of Figure 2 (c) (S = 10.0)

Figure 4 shows the variation in edge gradient with coherence for all classes of objects investigated.⁵ It is noted that as the object becomes less sharp the rate of change in the edge gradient with decreasing coherence shows a smaller magnitude. Nevertheless, the gradient still decreases most rapidly in the region from $\epsilon = 0.8$ to $\epsilon = 1.1$, and therefore it appears desirable for edge scanning to operate a microdensitometer with the ratio of numerical apertures of the illuminating objective to the analytical objective of 0.8. In this mode of operation it should be possible to increase the contrast and gradient of the edge traces without an increase in ringing.

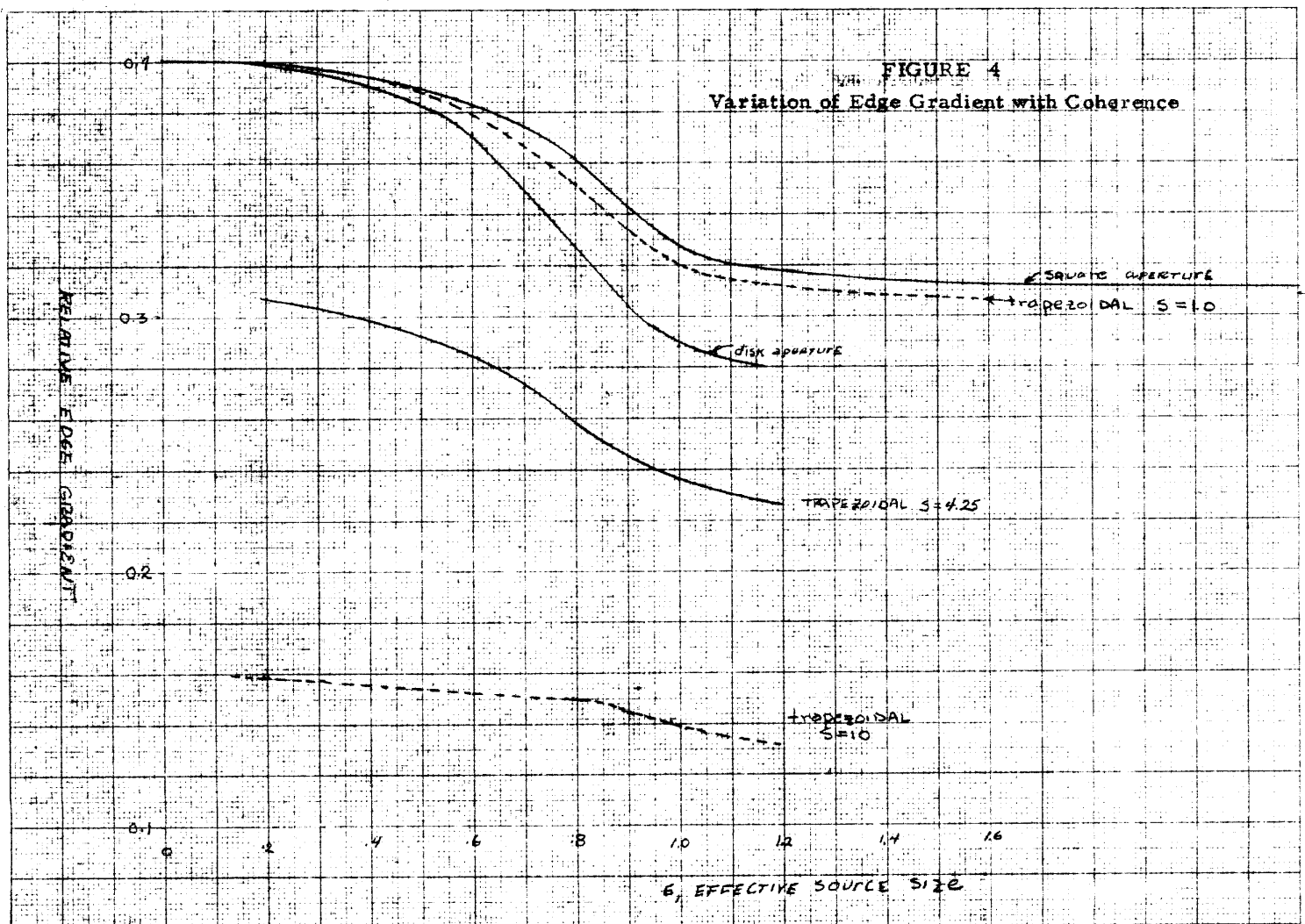
COMPARISON OF TECHNIQUES FOR DETERMINING A TRANSFER FUNCTION

In experimentally evaluating the modulation or contrast transfer function of an optical instrument, it is customary to employ edge or sine wave inputs. Since the system (in particular a microdensitometer) is not completely incoherent, the problem was to determine the expected theoretical results from such measurements of the transfer function. In employing edge inputs the problem was answered simply by taking the existing theoretical edge images previously computed and using them as inputs to the existing computer program for determining the transfer functions from edge traces. This was done for the square aperture - rectangular object edge with $\epsilon = 1.0$ (matched aperture), for the disk aperture - rectangular object edge with $\epsilon = 1.0$ and 0.8, for the trapezoidal object with $S = 1.0$ and matched objectives and for the incoherently illuminated edge. The resulting modulation transfer functions are shown in Figures 5 (a), (b), and (c).

The transfer functions are plotted for a numerical aperture of 0.4 (20X objective) only as a matter of convenience. If other numerical apertures are employed, the frequency scale must be decreased or increased in a direct proportion to the numerical aperture. In Figure 5 (a) the rectangular aperture shows a high MTF than the disk aperture, as is expected since it yields higher edge gradients. The transfer function for the disk matched aperture ($\epsilon = 1.0$) possess a lower modulation than the unmatched disk apertures ($\epsilon = 0.8$) for frequencies below 1000 lines/mm and a higher modulation for frequencies above 1100 lines/mm. Since the image of the edge is sharper when

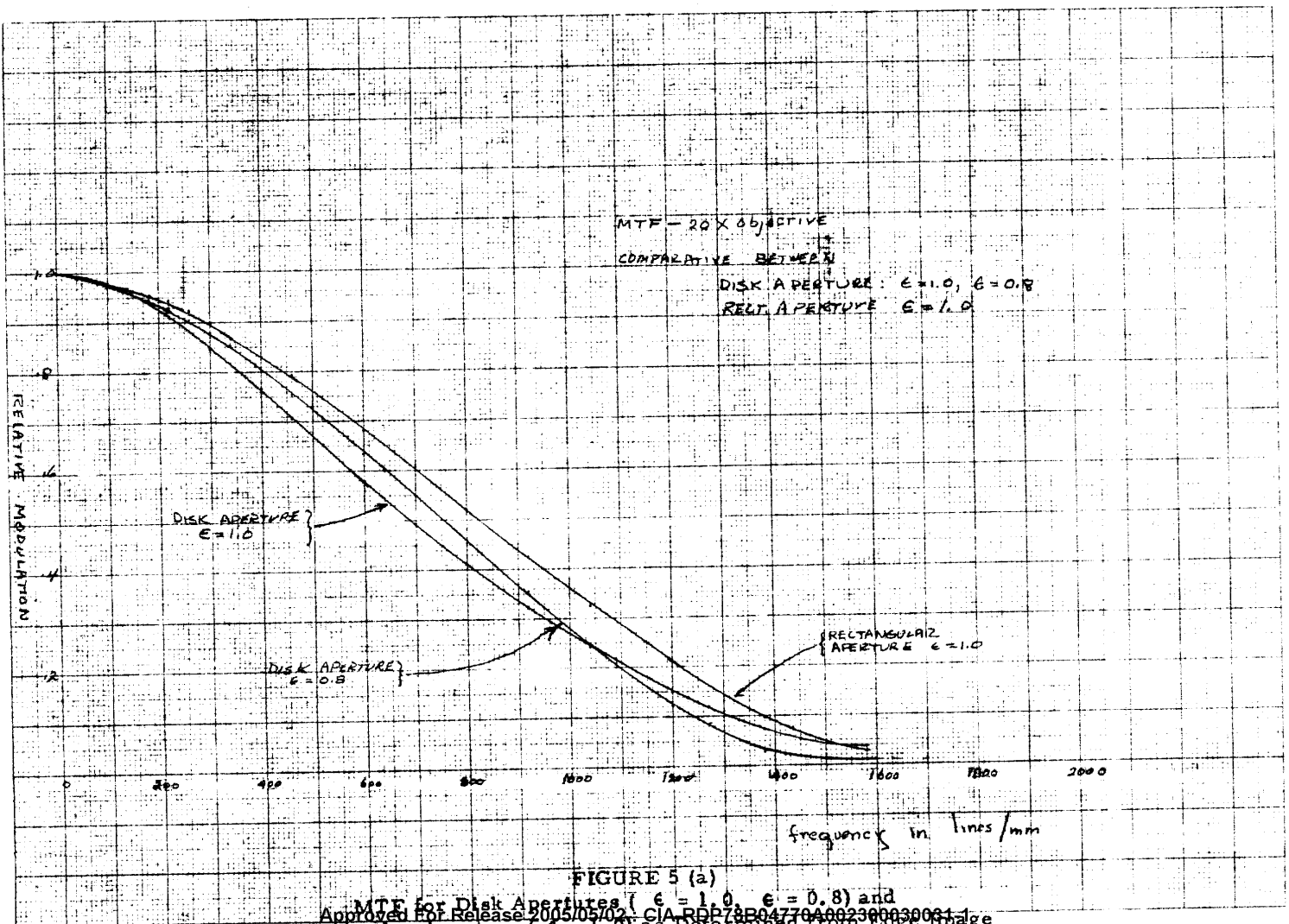
⁵ The investigations of rectangular objects with disk apertures instead of square apertures were carried out under the internal research program. The significant difference between square and disk apertures is that the corresponding curves for the same degree of coherence exhibit a larger edge gradient in the case of the square aperture. This result can be seen in the figure.

Approved For Release 2005/05/02 : CIA-RDP78B04770A002300030031-1



Approved For Release 2005/05/02 : CIA-RDP78B04770A002300030031-1

Approved For Release 2005/05/02 : CIA-RDP78B04770A002300030031-1



Approved For Release 2005/05/02 : CIA-RDP78B04770A002300030031-1

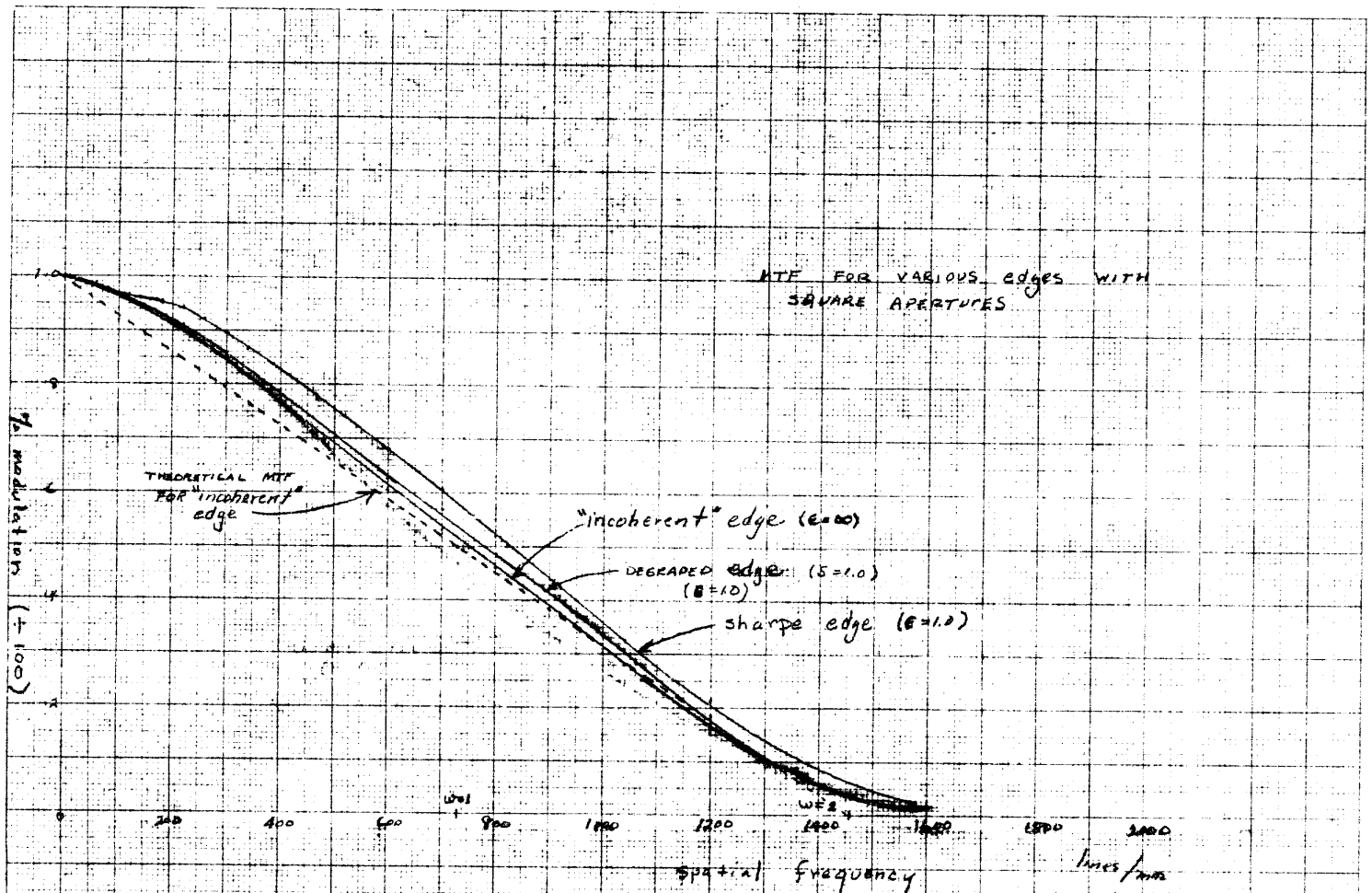
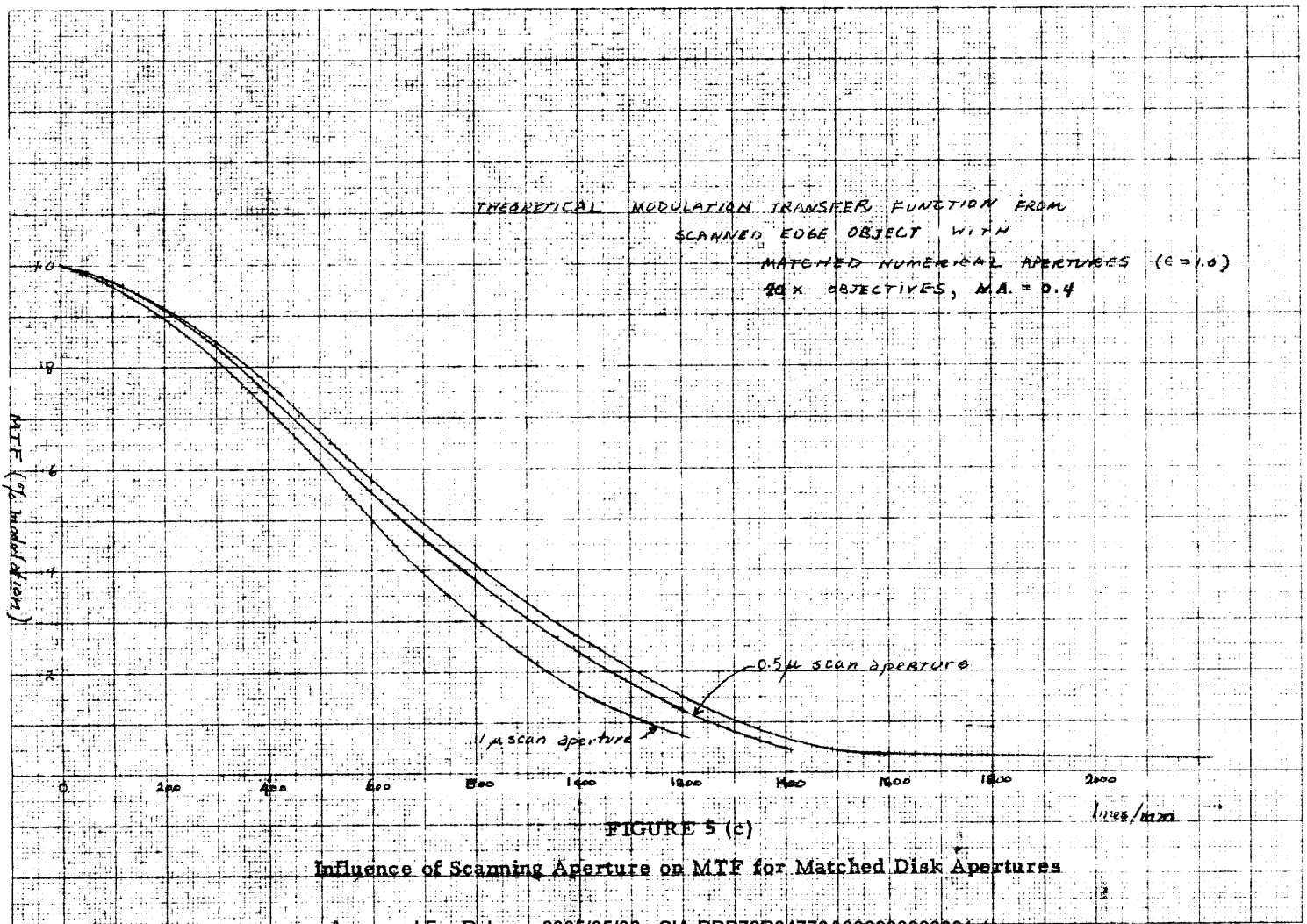


FIGURE 5 (b)

Comparison of MTF Determined from Sharp Edge ($\epsilon = 1.0$, $\epsilon = \infty$) and Degraded Edge ($S = 1.0$)

Approved For Release 2005/05/02 : CIA-RDP78B04770A002300030031-1



Approved For Release 2005/05/02 : CIA-RDP78B04770A002300030031-1

$\epsilon = 0.8$ than when $\epsilon = 1.0$, the conclusion that a system which has a higher MTF at high frequencies will produce sharper edges is not necessarily valid. Figure 5 (b) shows the transfer functions determined from the images of the incoherently illuminated edge, the matched aperture cases for the sharp edge (rectangular object) and degraded edge (trapezoidal object). The dashed curve is the theoretical incoherent transfer function for a square aperture. It is a straight line passing through 0.5 at $\omega = 1$ (~ 728 lines/mm). The MTF labeled "incoherent edge" should agree exactly with the dashed line. The fact that it does not arises from the error in the numerical computation technique used in computing transfer function from edge traces. In addition, both the sharp edge and the slightly degraded edge yield higher modulations than the incoherent limit (compared to MTF from incoherent edge). The sharp edge MTF exceeds the incoherent limit by 5% - 30% and the degraded edge MTF exceeds the incoherent limit by 1% - 10% for frequencies below 600 lines/mm. Therefore, the fact that one cannot achieve a sharp edge for testing optical instruments using partially coherent illumination may be an advantage in that the expected result for a degraded edge may be closer to the incoherent diffraction limit than the result for the sharp edge.

Figure 5 (c) also shows the MTF determined from the image of a sharp edge with matched disk apertures. The other curves represent the influence of the scanning aperture which was not included in the results present in 5 (a) or 5 (b). The influence of the scan aperture is taken into account by convolving it with the edge image before finding the MTF or equivalently by multiplying the MTF by $\frac{\sin \pi \omega}{\pi \omega}$ where $\omega = \frac{\text{spatial frequency (lines/mm)}}{W_s \text{ (mm)}}$ and W_s = width of the scanning slit.

In order to examine sine-wave inputs for computing the incoherent transfer function of microdensitometers, it is assumed that the intensity transmittance of the object is given by:

$$T_I(u) = K + \cos \omega u \quad |u| < \infty, K \geq 1$$

where u is the reduced coordinate in the image plane and $\omega = (\text{spatial frequency}) \times (\text{wavelength of light}) / \text{numerical aperture}$. The image is examined by employing an identical procedure as that used in the case of the edged objects reported in this and the previous memo. The object amplitude spectrum is given by:

$$O(m) = \frac{1}{2\pi} \int_{-\infty}^{\infty} (K + \cos \omega u)^{1/2} e^{-im u} du \quad (4)$$

This is a form of an elliptical integral and does not possess a closed form solution. Consequently, the approximation is made that:

$$(K + \cos \omega u)^{1/2} \approx K \left(1 + \frac{1}{2K} \cos \omega u - \frac{1}{8K^2} \cos^2 \omega u + \frac{1}{16K^3} \cos^3 \omega u \right) \quad (5)$$

and one finds that:

$$\alpha(m) = C_0 \delta(m) + C_1 [\delta(m+\omega) + \delta(m-\omega)] + C_2 [\delta(m+2\omega) + \delta(m-2\omega)] + C_3 [\delta(m+3\omega) + \delta(m-3\omega)] \quad (6)$$

where

$$\begin{aligned} C_0 &= 1 - \frac{1}{16K^3} & C_2 &= -\frac{1}{32K^2} \\ C_1 &= \frac{1}{4K} + \frac{3}{128K^3} & C_3 &= \frac{1}{128K^3} \end{aligned}$$

Again, by employing (6) and performing two integrations, one may arrive at the intensity distribution for the image. The modulation transfer function is determined by taking the maximum and minimum intensities in the image and substituting them into:

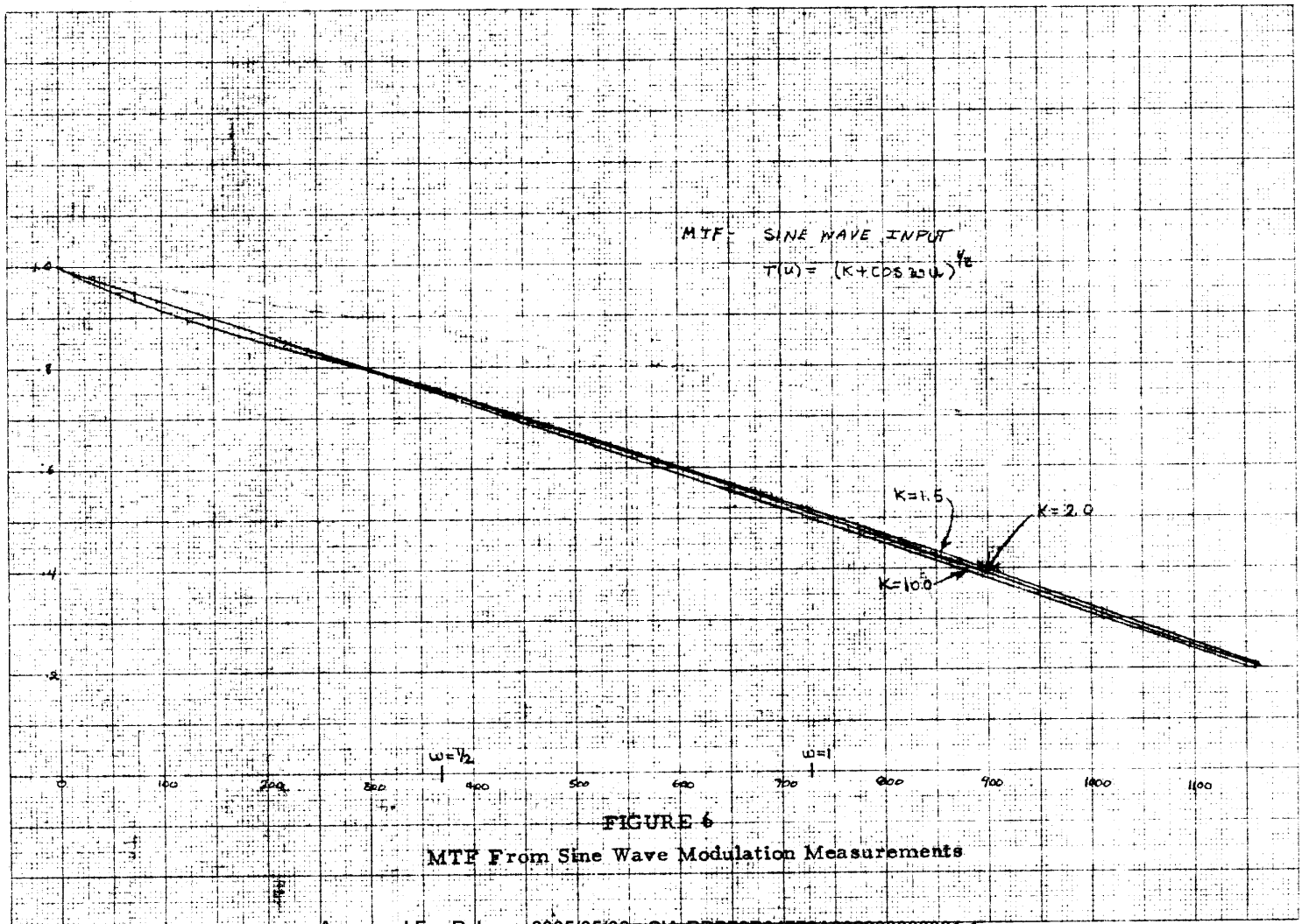
$$MTF(\omega) = \frac{K(I_{max} - I_{min})}{I_{max} + I_{min}} \quad (7)$$

It is observed that the intensity distribution of the image for $1 \leq \omega \leq 2$ is of the form

$$I'(u') = K' + \cos \omega u'$$

but in the region of $0 \leq \omega \leq 1$, the distribution distorts from a sinusoidal wave between successive maxima and minima. The resulting MTF (ω) for various values of K are shown in Figure (6). It is noted that all the curves follow very closely to the expected incoherent limit (line passing through 1.0 at $\omega=0$ and 0.5 at $\omega=1$), in fact the curve for $K = 10.0$ is indistinguishable from the incoherent limit. The reason for the better agreement compared to the theoretical incoherent transfer function in the case of the sine-wave objects is simply that the distortion of the image produced by employing matched aperture rather than a more incoherent illumination does not affect the relative maximum and minimum intensities and consequently, does not appreciably change the measured modulation. In the case of edge traces, distortion in the image is reflected by a change in the MTF because it is dependent upon the intensity distribution in the image, not at a few points, as in the case of the sine-wave images.

Approved For Release 2005/05/02 : CIA-RDP78B04770A002300030031-1



Approved For Release 2005/05/02 : CIA-RDP78B04770A002300030031-1

Finally, one point which may already be obvious to the reader is that although one may measure the incoherent transfer function (even when the system is using partially coherent illumination of the object) by employing appropriate objects (objects with sine-wave intensities appear to be best) the application of this derived transfer function to determine the intensity distribution to other objects employed in the system is in general not valid.

Coherent Illumination (Laser Source)

The problems investigated here concerns the effect upon edge traces caused by employing coherent illumination in the microdensitometer (e.g., laser source) and by decreasing the illuminating slit dimensions. When the illuminating slit is wide enough to image the edge objects in the image or scanning plane (this is the usual way the microdensitometer system is employed), the influence of employing coherent illumination upon the intensity distribution⁶ has already been determined. (See previous memo, Figure 5) The problem, therefore, is to determine the change in the edge trace when a coherent source is employed with a narrow (but finite) illuminating slit. The method of analysis employed in this investigation differs from the Hopkins' coherence theory used earlier. Previously, it was assumed that the light passing through the illuminating condenser was incoherent. In the case of a coherent light source, this illumination will be coherent so that another method of analysis must be employed. This method will be outlined briefly below.⁷

The propagation of the mutual intensity function through a plane which contains a modulating object whose amplitude transmittance is given by $T(x)$ can be shown to be given by the expression

$$I_{\text{after}}(x_1, x_2) = I_{\text{before}}(x_1, x_2) T(x_1) T^*(x_2) \quad (8)$$

Recalling Equation (1) of the previous memo for the propagation of the mutual intensity between successive planes which are relatively Fraunhofer,

$$I(x_1, x_2) = K \iint I(\xi_1, \xi_2) e^{i(x_2 \xi_2 - x_1 \xi_1)} d\xi_1 d\xi_2 \quad (9)$$

⁶ The term edge trace refers to the output of the microdensitometer when the intensity distribution is scanned by given effective aperture. Consequently, the term intensity distribution implies that the influence of the scanning aperture has not been taken into account.

⁷ Since the system is completely coherent, one could propagate the complex amplitude. However, the more general approach (for any degree of coherence) is to propagate the mutual coherence function. In the limit of complete coherence both techniques are identical.

one has the necessary tools to propagate the mutual intensity through an optical system. Consider the optical system shown in Figure 7 below.

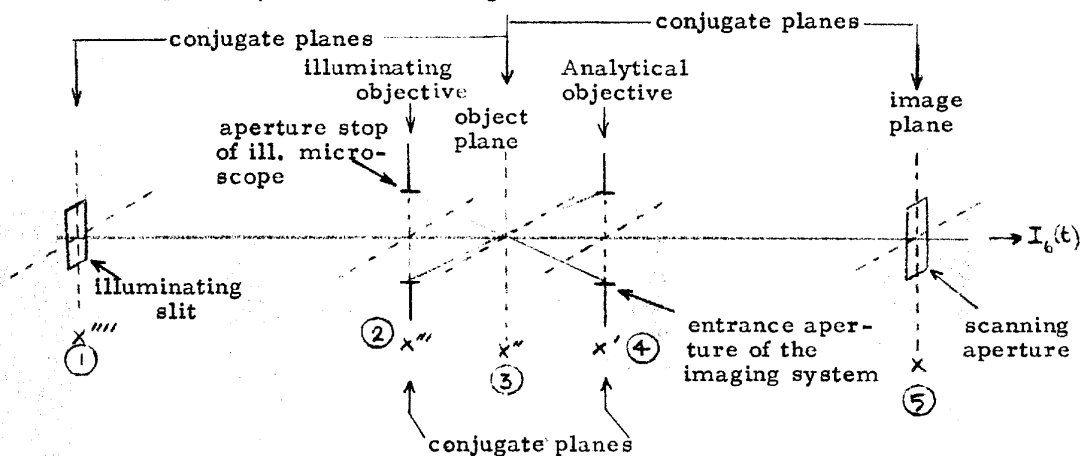


FIGURE 7
Microdensitometer System⁸

Let $2m$ = effective width of the illuminating slit (i.e. decreased by the magnification of the microscope)
 2α = effective width of the scanning slit
 $2a$ = width of system objectives (assumed to be equal for both the illuminating and analytical objectives)

where all of these widths are assumed to be expressed in reduced coordinates. Using Equations (8) and (9) to propagate the mutual intensity from planes ① to ②, ② to ③, etc., one may determine the mutual intensity function over the scanning slit, and, consequently, the intensity recorded by the photomultiplier. It will be assumed that the object in plane ③ is an edge and that it is moving in time so that the object amplitude transmittance can be described by:

$$T_3(x'', t) = \begin{cases} 1 & x_0 - st < x'' < \infty \\ 0 & \text{otherwise} \end{cases} \quad (9)$$

where x_0 is the relative location of the edge at $t = 0$. The transmittances of the stops or slits in the other planes are assumed to be:

⁸ It has been assumed throughout the analysis that the illuminating objective plane and the analytical objective plane are conjugate plane. This assumption will be discussed in more detail in the last section of this memo.

$$\begin{aligned}
 T_1(x''') &= \begin{cases} 1 & |x'''| \leq m \\ 0 & \text{otherwise} \end{cases} && \text{(illuminating slit)} \\
 T_2(x''') &= \begin{cases} 1 & |x'''| \leq a \\ 0 & \text{otherwise} \end{cases} && \text{(illuminating objective assumed to be the aperture stop of the illuminating system)} \\
 T_4(x') &= \begin{cases} 1 & |x'| \leq a \\ 0 & \text{otherwise} \end{cases} && \text{(analytical objective is assumed to be aperture stop of the imaging system)} \\
 T_5(x) &= \begin{cases} 1 & |x| \leq L \\ 0 & \text{otherwise} \end{cases}
 \end{aligned}$$

The resulting expression for the intensity recorded on the photomultiplier, $I_6(t, m, \alpha)$, is given by

$$I_6(t, m, \alpha) = \int_{-L}^L \left\{ \int_{u(t)}^{\infty} \frac{\sin(\gamma + \alpha)}{\gamma + \alpha} [S_i(\gamma + m) - S_i(\gamma - m)] d\gamma \right\}^2 d\alpha \quad (10)$$

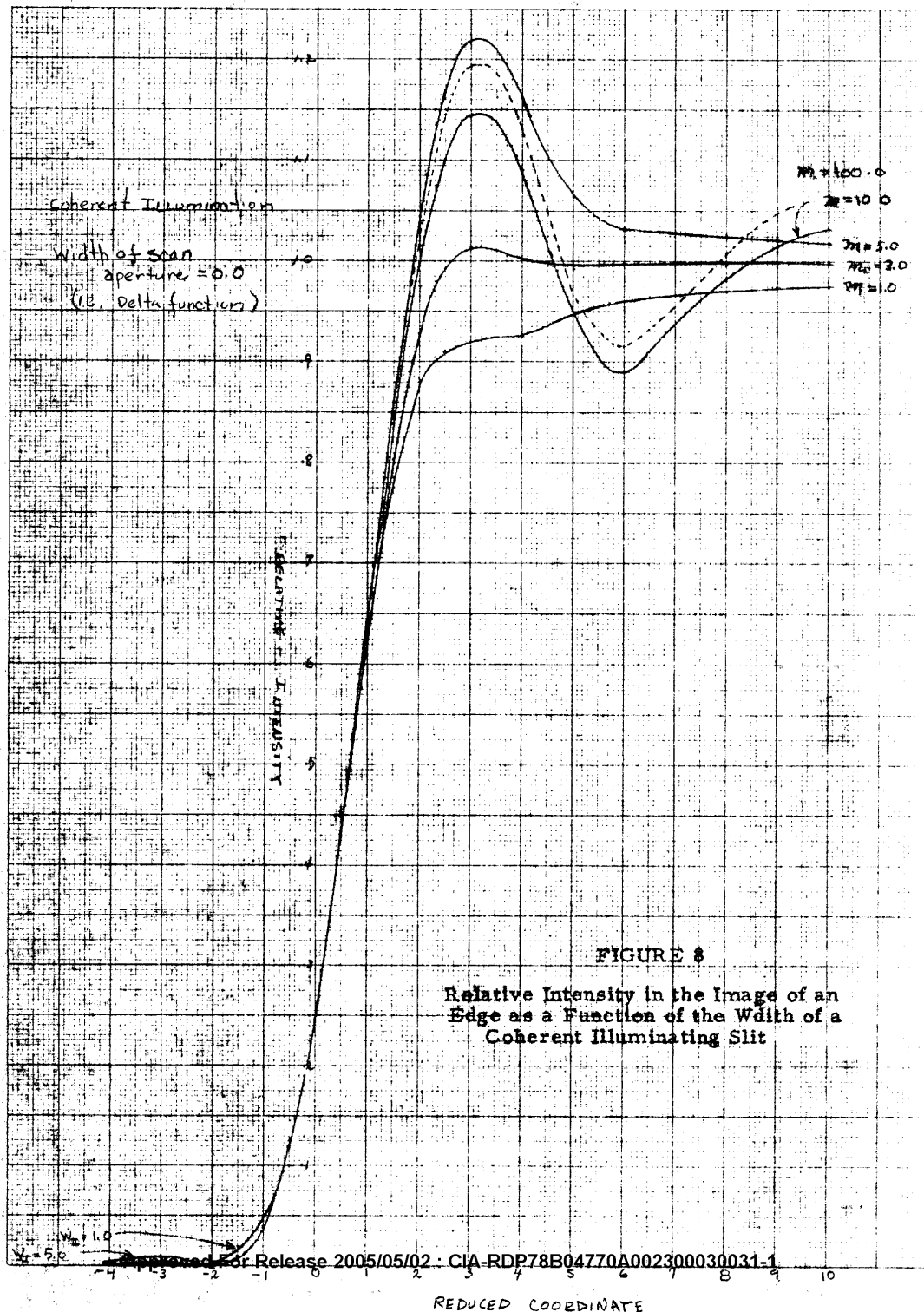
where $\gamma = a x''$, $\alpha = a x$ and $u(t) = a(x_0 - st)$

Note that $u'(t) = 0$ is the "image" coordinate conjugate to the edge of the object. Equation (10) was solved by using an IBM 7044. The upper limit of integration on γ (i. e., infinity) can be relaxed since the integrand decreases very rapidly with increasing γ $[O(\frac{1}{\gamma^3})]$. The choice of the upper integration limit is dependent upon the value of L (half-width of the scanning slit). It was decided to set the limit equal to $20\pi + L$.⁹ Figure 8 contains the intensity distribution of the image for values of $m = 1.0, 3.0, 5.0, 10.0$, and 100.0 for an infinitesimal width scanning slit. The distributions all pass through 0.25 at $u' = 0$. Initially ($m = 1.0$), there is no ringing in the image. As m is increased ($m = 3.0$), the image becomes sharper (i. e., larger gradient) and the ringing increases. At $m = 5.0$ the first maximum in the bright side of the image is visible. Further increase in the illuminating slit ($m = 10.0$) causes the first "minimum or dark fringe" to appear. Additional increases in the slit width consequently cause the distribution to approach the coherent diffraction pattern of an edge which is to be expected. At $m = 100.0$ the pattern is identical (less than 1/2% of deviation) to the coherent diffraction pattern (for infinite illuminating slit) over the range of u' shown in the figure. It is interesting to note that when $m = 3.0$,

⁹ At first the upper integration was set equal to $10\pi + L$, the change in intensity occurring when the limit was set at $20\pi + L$ was found to be small (less than 1/2%).

VISIGRAPH
MADE IN U.S.A.

NO. 1578 MP GRAPH PAPER
MILLIMETER



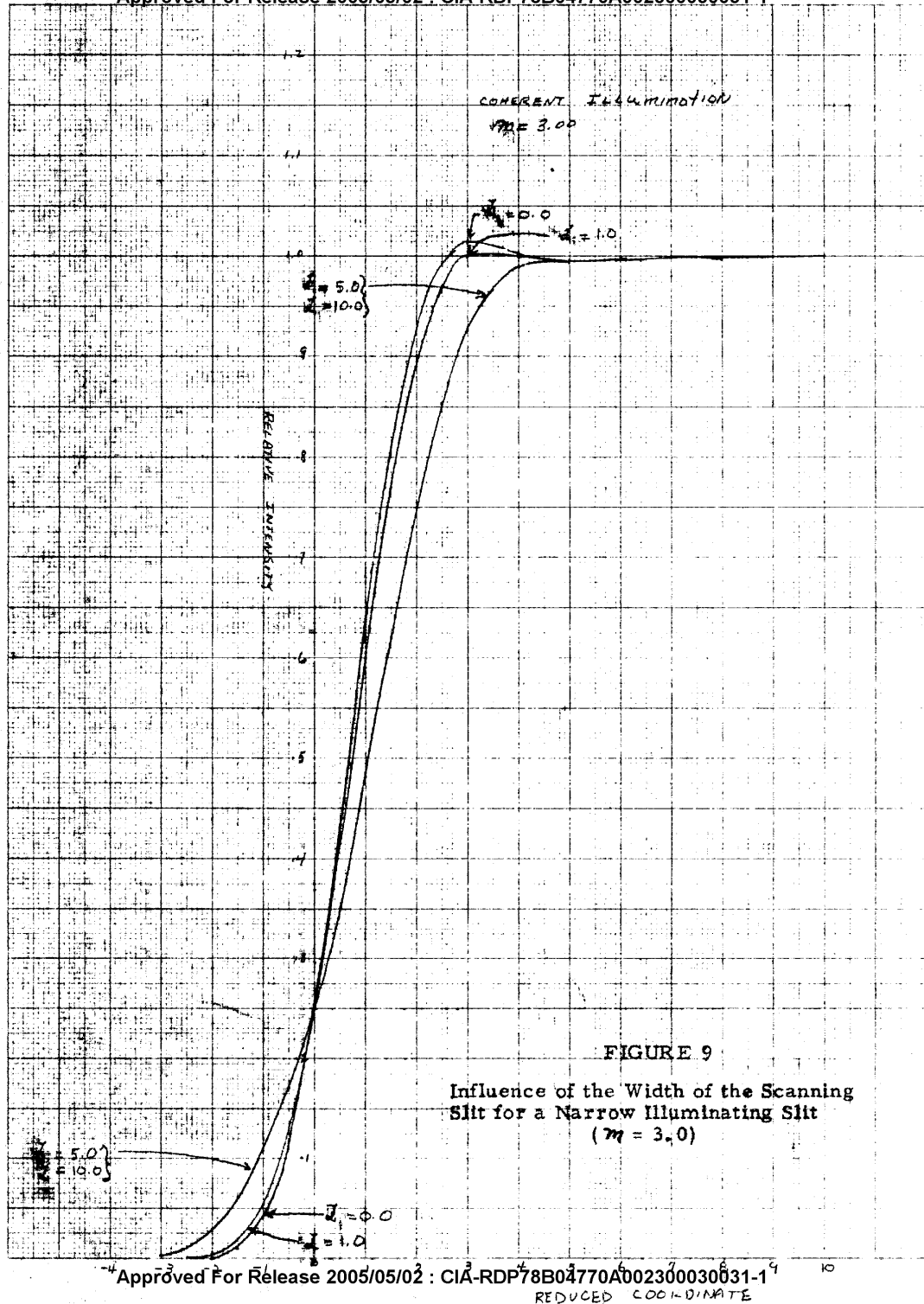
the intensity distribution has the highest gradient possible without possessing large ringing. Consequently, Figure 9 was plotted showing the influence of increasing, \mathcal{L} , the width of the scanning aperture when $m = 3.0$. It is noticed that the initial increase in the width produces a result which resembles the convolution of the image when $\mathcal{L} = 0$ with the scanning aperture. However, once $\mathcal{L} \geq 5$ only very small changes in the intensity distribution in the image occur when the width of the scanning aperture is increased. This simply indicates that once $\mathcal{L} = 5.0$, the photomultiplier is collecting all the light available in the "image". This indicates that unless the scanning slit is small (equal to or less than the illuminating slit) it can be eliminated from the system for narrow illuminating slits (although the slit probably is desirable in practice, to eliminate stray light).

Figure 10 shows an expanded scale for \mathcal{U}' between -1.0 to +2.0 of Figure 9 and is presented in order to show the decrease in edge gradient with increasing width of the scanning slit for the $m = 3.0$ image.

CONCERNING THEORETICAL ASSUMPTIONS

The theoretical analysis presented in this and a previous memo have assumed that the illuminating objective and the analytical objective lie in conjugate planes. For example, when the tungsten light bulb is employed as the light source in the microdensitometer system to illuminate a slit large compared to the airy disk of the illuminating objective, it can be shown¹⁰ that the objective aperture is incoherently illuminated and can be considered the effective source of the system. This condition usually exists. However, the formulation of coherence theory developed by [redacted] and employed in part of the analysis also requires that the effective source is imaged in the entrance aperture of the imaging system or, in the case of the microdensitometer, that the illuminating objective (effective source) and the analytical objective (entrance aperture) lie in conjugate planes. This assumption was also made in the previous section, as indicated in Figure 7. In order to justify this assumption, imagine that a hypothetical lens exists just after the object plane in Figure 7 which images the condenser aperture into the entrance aperture. For coherent illumination this means that the object spectrum is formed in the entrance aperture. In order to compensate for the influence of the hypothetical lens upon the object (i. e., the light beyond the object must be distributed as it is without the fictitious lens), assume that the object transmittance includes a compensating phase factor which is given by $e^{i\phi(u)}$

¹⁰ M. Born and E. Wolf, "Principles of Optics," (Pergamon Press, 1964), pp. 518-520.
S. C. Som, Optica Acta, 10, 179.

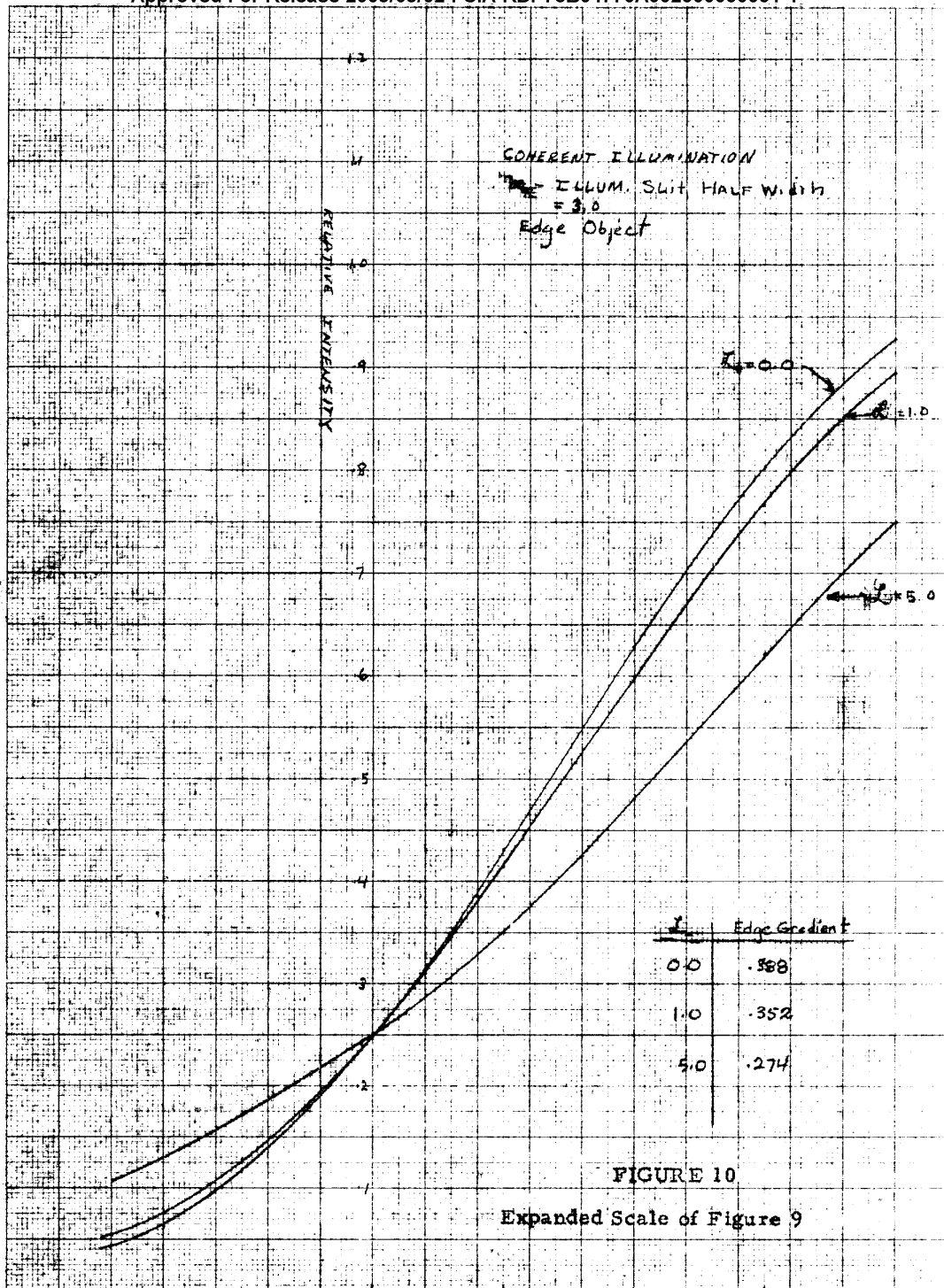


VEICGRAPH
MADE IN U.S.A.

NO INSTR. OR GRAPH PAPER
MILLIMETER

VEICGRAPH
MODEL 10-1-1

NO 157R AIR GRAPH PAPER
MIL. LINE PER



where:¹¹

$$\phi(u) = \frac{1}{2kf} \frac{u^2}{(N.A.)_o^2}$$

$(N.A.)_o$ - numerical aperture of the analytical objective

f - focal length of hypothetical lens

$k = 2\pi/\lambda$

u - reduced object coordinate

When the numerical apertures of the analytical objective and the condenser are matched,

$$\frac{1}{2f} = \frac{1}{W}$$

where W = working distance of the objectives.

So

$$\phi(u) = \frac{\lambda}{2\pi(N.A.)_o^2 W} u^2 = 2\pi K u^2$$

$$K = \frac{\lambda}{4\pi^2(N.A.)_o^2 W}$$

In order to determine the magnitude of $\phi(u)$ consider the following typical values for microscope objectives:¹²

$(N.A.)_o$ Numerical Aperture	W Working Distance	$W(N.A.)_o^2$
.1	38 mm	3.8×10^{-2} cm
.25	7	4.4×10^{-2} cm
.50	1.6	4.0×10^{-2} cm
.85	0.2	1.4×10^{-2} cm

It is seen that $W(N.A.)_o^2 \sim 4.0 \times 10^{-2}$ cm and when $\lambda = 5.5 \times 10^{-5}$ cm:

$$\frac{\lambda}{4\pi^2} = 1.4 \times 10^{-6} \text{ cm}$$

so that:

$$K = 3.5 \times 10^{-5}$$

¹¹ [redacted] Report No. VE-1522-G-1, 13 February 1962, p. I.3, Equation (I.3).

¹² A. Hardy and F. Perrin, "The Principles of Optics," (McGraw-Hill, 1932) p. 501,

For values of $|u| < 50$ the phase correction factor is less than $(1/10)\lambda$.

When the usual tungsten source is employed, the phase factor is essentially constant over the coherence length ($\Delta u \sim 10$) and can be neglected. In the case of the laser source the previous investigations entailed illuminated areas in the object plane for which $|u| \leq 50$ so that the phase factor can similarly be neglected. Consequently in both cases it is reasonable to assume that the condenser and analytical objective lie in "conjugate planes". This conclusion is not valid when the coherent source is employed with a wide illuminating slit. In this case the compensating phase factor should be included in the object, unless only narrow image fields are of interest.

RECOMMENDATIONS FOR FUTURE WORK

Investigations should be made for other amplitude objects and for phase objects. In addition, a more intensive study should be made of the illuminating system including the possibility of employing phase apertures to "improve" the image intensity distributions and also the effects produced by employing partially coherent illumination of narrow illuminating apertures.



STAT